Bioorg. Med. Chem. Lett.

Split luciferase-based estimation of cytosolic cargo concentration delivered intracellularly via attenuated cationic amphiphilic lytic peptides

Syusuke Okano, Yoshimasa Kawaguchi, Kenichi Kawano, Hisaaki Hirose, Miki Imanishi, Shiroh Futaki*

Institute for Chemical Research Kyoto University, Uji, Kyoto 611-0011, Japan

*Corresponding author
Tel: +81-774-38-3210. Fax: +81-774-32-3038. E-mail: futaki@scl.kyoto-u.ac.jp.

Highlights

1. Measurement of actual cytosolic concentrations aids design of effective cellular delivery methods.
2. A split-NanoLuc luciferase system to estimate and compare efficacy of cytosolic cargo delivery.
3. Membrane permeabilizing peptides L17E and HAad increase efficiency of intracellular delivery by 6-fold.

Abstract

Intracellular delivery of biomacromolecules is challenging as these molecules are taken up by cells and encapsulated into vesicular compartments called endosomes, and the fraction of molecules that are translocated to the cytosol are particularly important to obtain desired biological responses. This study aimed to estimate the cytosolic concentrations of intracellularly delivered peptides and proteins to aid the design of novel and effective biopharmaceutical delivery systems. To this end, we employed the split NanoLuc luciferase system, using the 11-residue HiBiT peptide segment as a probe for the delivered molecules in cells expressing the complementary LgBiT protein segment. The efficacy in cytosolic HiBiT delivery was determined by measuring the resultant luciferase activity when the HiBiT segment delivered into the cytosol forms a complex with LgBiT. Mean cytosolic HiBiT concentration was calculated using cell number and cell volume analysis. L17E and HAad peptides, developed in our laboratory for intracellular protein delivery, yielded approximately 6-fold higher cellular HiBiT concentrations than that obtained in their absence.

Keywords (5)
intracellular delivery; endosomal release; cytosolic concentration; split-NanoLuc luciferase assay; attenuated cationic amphiphilic lytic (ACAL) peptide

Abbreviations

CPPs: cell-penetrating peptides
ACAL: attenuated cationic amphiphilic lytic
GABA: γ-aminoburyric acid
CLSM: confocal laser scanning microscopy
DIC: differential interference contrast
HPLC: high-performance liquid chromatography

Intracellular delivery of biomacromolecules, including peptides and proteins, is one of the most demanding challenges in chemical biology, medicinal chemistry, drug delivery, and related research fields.[1-3] The cell membrane (plasma membrane) is generally impermeable to these biomacromolecules, and endocytic pathways are typically utilized as delivery routes.[4-6] The cargo biomacromolecules taken up by cells are encapsulated by vesicular compartments (i.e., endosomes) (Figure 1). The desired activities and functions of these cargo molecules can only be achieved if the molecules are released from the endosomal vesicles into the cytosol. Therefore, approaches and strategies to facilitate the cellular uptake and endosomal release of cargo molecules have been developed, including the use of lipid/polymer-based nanoparticles, cell-penetrating peptides, and structurally constrained peptides.[7-10] In addition, our laboratory is currently developing approaches for intracellular delivery using cell-penetrating and membrane-permeabilizing peptides, including attenuated cationic amphiphilic lytic peptides such as L17E[11] and HAad,[12] to efficiently deliver antibodies [immunoglobulin G (IgG), approximately 150 kDa] and other bioactive proteins to live cells.[2,13,14]

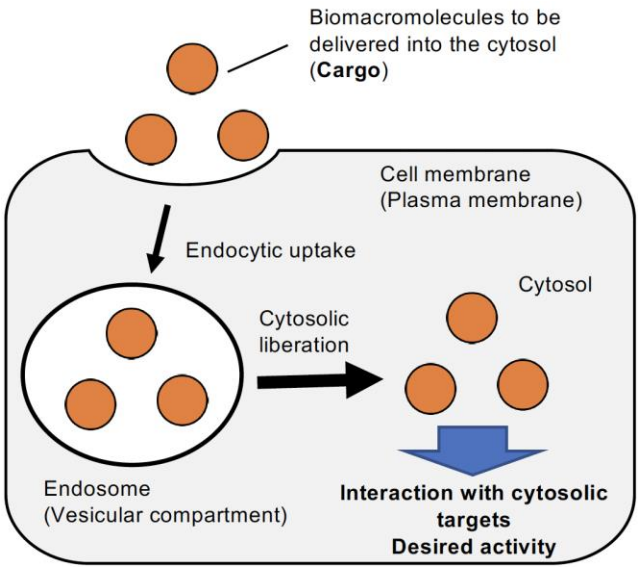

Figure 1. Endosomal release is needed to obtain the desired activity in intracellular (i.e., cytosolic) delivery of biomacromolecules via endocytosis.

Systems for evaluating the efficacy of cytosolic cargo delivery are essential in the development of intracellular delivery systems. The representative methods used for this purpose include flow cytometry analysis[15] and mass spectrometry.[16] However, these methods analyze the cargo amount of total cellular uptake, which also includes fractions of endosome-trapped cargos to be released into the cytosol in addition to the fraction actually reaching the cytosol. Microscopic analysis of the cellular localization of fluorescently labeled cargo molecules is also frequently employed.[15] This method is rather qualitative, and the precise estimation of cytosolic cargo concentration is generally difficult, particularly when the concentrations is low. A more reliable way to evaluate delivery efficacy is to analyze the cytosolic activity of cargo biomacromolecules.[17] In this regard, quantification methods for evaluation of cytosolic cargo fractions have been developed,[4] such as the reconstitution of split fluorescent proteins,[18-20] split luciferases,[21] and other fluorogenic protein segments.[22] Additional approaches include the use of fluorescence moieties that gain intensity via modification by cytosolic enzymes or alteration in the chromophore environment[23-27] and the use of fluorescence correlation spectroscopy (FCS) for the analysis of cytosolic peptides.[28] However, these assays only allow evaluation of the relative efficacy of delivery methods and the actual cytosolic concentrations of cargo molecules attained by these methods cannot be gauged. Considering that each cargo has a preferred concentration range to exert its activity in the cytosol and avoid possible cytotoxicity, information on cytosolic cargo concentrations is highly valuable for the design of biopharmaceutics and delivery systems. Thus, novel approaches are required to estimate the actual cytosolic concentration of the delivered cargo. This study aimed to develop an approach to estimate the cytosolic concentration of intracellularly delivered cargo and investigate the abilities of delivery peptides developed in our laboratory.

To achieve our aim, we designed a system using the NanoLuc split-luciferase assay (Figure 2A). This split luciferase system comprises the HiBiT segment, an 11-residue peptide segment (sequence: VSGWRLFKKIS), that binds to its counterpart LgBiT fragment (approximately 18 kDa) with high affinity (K_d = 700 pM).[29] The split luciferase system evaluates intracellular interactions based on high binding activity and is utilized for analyzing protein-protein interactions in live cells.[30] Therefore, the cytosolic release of cargo peptides and proteins can be monitored via live-cell luciferase assay using HiBiT-tagged cargos and LgBiT-expressing cells (i.e., LgBiT present in the cytosol but not in endosomes). This assay system was also employed by Teo et al. for comparing intracellular delivery efficacies of cell-penetrating peptides (CPPs).[21]

However, the efficacies were evaluated in terms of the relative cytosolic cargo uptake amount without focusing on the actual cytosolic concentration of the delivered cargo.

The LgBiT/HiBiT split-luciferase system can be employed not only in live cells but also in cell lysates. We should herein consider possible differences in the luminescence generated by the LgBiT/HiBiT complex under both conditions. The analysis of the correlation of luminescence generated under the two conditions yielded a correction coefficient $\boldsymbol{X}/\boldsymbol{Y}$ in Figure 2B. Meanwhile, the relationship between luciferase activity and HiBiT concentration in cell lysates was obtained by adding a known amount of HiBiT substrate in the presence of LgBiT, yielding the slope $\boldsymbol{k}$ in Figure 2C. Subsequently, cytosolic HiBiT concentration in live cells was calculated assuming that most of the HiBiT segment-bearing cargos formed complexes with LgBiT in the cytosol. We then analyzed the number and volume of cells, corresponding to $\boldsymbol{n}$ and $\boldsymbol{V}$ in Figure 2D, respectively, to obtain a rough estimation of the cytosolic concentration of the delivered cargo.

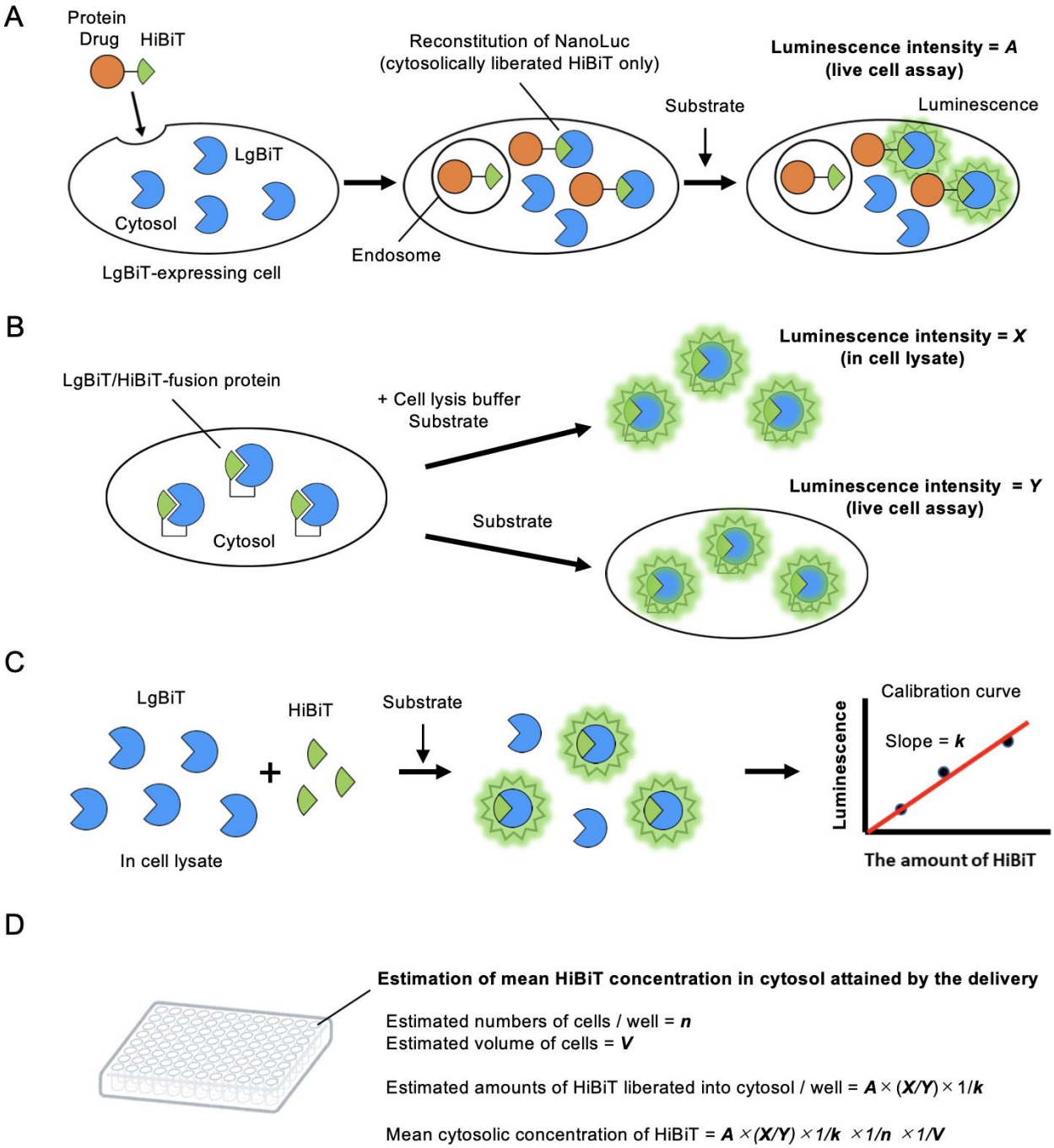

Figure 2. Designed system for analyzing cytosolic concentration of cargo molecules. (A) NanoLuc split-luciferase assay system for the detection and quantification of cargo molecules released into the cytosol. (B) Differences in the luminescence generated by the LgBiT/HiBiT complex between live cells and cell lysates. (C) Standard curve generation for cell lysates. (D) Estimation of cytosolic cargo concentration.

To confirm that the employed HiBiT peptides *per se* had little cytosolic appearance and that the presence of delivery peptides L17E[11] and HAad[12] caused a stimulation of the cytosolic delivery of HiBiT peptides, we analyzed cellular localization of the intracellularly delivered HiBiT peptides using confocal laser scanning microscopy (CLSM).[12] Although HiBiT is widely used as a peptide probe it contains hydrophobic (V, W, L, F, I) and basic (R, K, K) amino acids, and such peptides are often membrane-permeable.[23,31] Ideally, model cargos of very low membrane permeability should be used for evaluating cellular internalization. Therefore, we employed the model peptide cargo 2RD-HiBiT, bearing a hydrophilic RDRDR sequence, and a fluorescein isothiocyanate (FITC) label to allow CLSM analysis at its N-terminus (Figure 3A). In the absence of L17E and HAad, FITC-2RD-HiBiT predominantly yielded dot-like punctate signals within the cells, suggesting endocytic uptake of FITC-2RD-HiBiT (Figure 3B). Based on the lack of substantial diffuse FITC-2RD-HiBiT signals in the cytosol, it was evident that most FITC-2RD-HiBiT was trapped in the endosomal vesicles and not released into the cytosol. In contrast, in the presence of L17E and HAad, a considerable cell fraction (approximately 50%) exhibited diffuse FITC-2RD-HiBiT signals throughout the cells, confirming the capabilities of L17E and HAad to facilitate cytosolic cargo delivery, as previously reported[11,12] (Figure 3B).

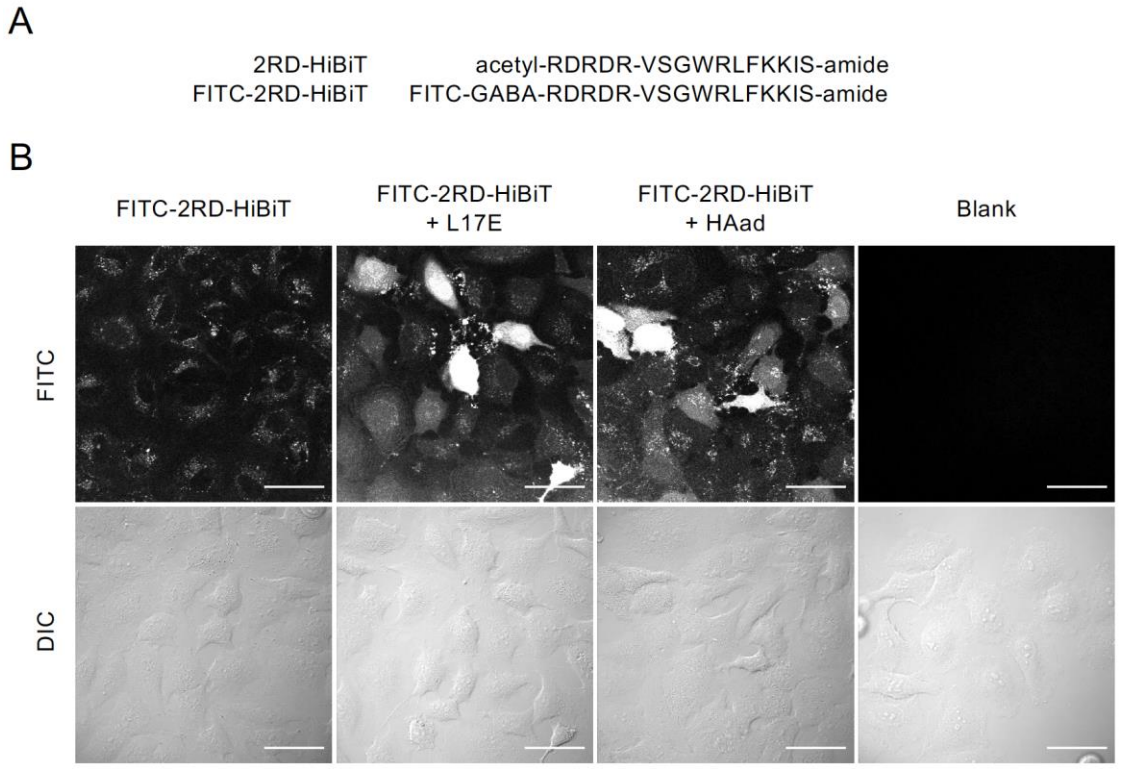

Figure 3. (A) 2RD-HiBiT and FITC-2RD-HiBiT structures. GABA (= γ-aminobutyric acid) was employed as a spacer to connect the FITC moiety with the peptide segment to avoid possible Edman-like degradation.[32] (B) Cellular distribution of FITC-2RD-HiBiT (5 μM) in the absence or presence of L17E and HAad (40 μM each) following a 30-min treatment. Scale bars, 40 μm.

As suggested in Figure 3, the concentration of 2RD-HiBiT delivered in cytosol should vary considerably in each cell. However, the information on the concentration ranges of cargos is important for the design of the delivery systems and the evaluation of the accompanied cellular activity. Therefore, we evaluated the mean concentration of cytosolic 2RD-HiBiT delivered via L17E and HAad, as illustrated in Figure 2.

We generated cells expressing a LgBiT-HiBiT fusion protein (Figure S1) and measured its luciferase activity using both live cell and cell lysate assays (Figure 2B). The ratio (***X/Y*** = 0.68) of the luminescence intensity values obtained from the former assay (***X***) to that from the latter assay (***Y***) was defined as the correction coefficient (see Supporting Information for experimental details). As illustrated in Figure 2C, the luminescence generated by the interaction between LgBiT and varying 2RD-HiBiT concentrations (0.2–2 nM) was analyzed using a cell lysate assay (see Supporting Information for experimental details). Subsequently, a linear correlation was obtained with a slope ***k*** of 6.6×10^{3} (a.u./fmol^{-1}), where a.u. represents the arbitrary unit of luminescence intensity (Figure 4). The volume of each cell was estimated using differential interference contrast (DIC) microscopy on HeLa cells (Figure S2). Assuming the cells to be spherical structures, we gauged the diameters of 15 cells using ImageJ software and obtained a value of 18 μm. From this, we calculated the volume of each cell (***V***) to be 3.2 pL and these values were then used to calculate the cytosolic concentration of 2RD-HiBit (Figure 2D).

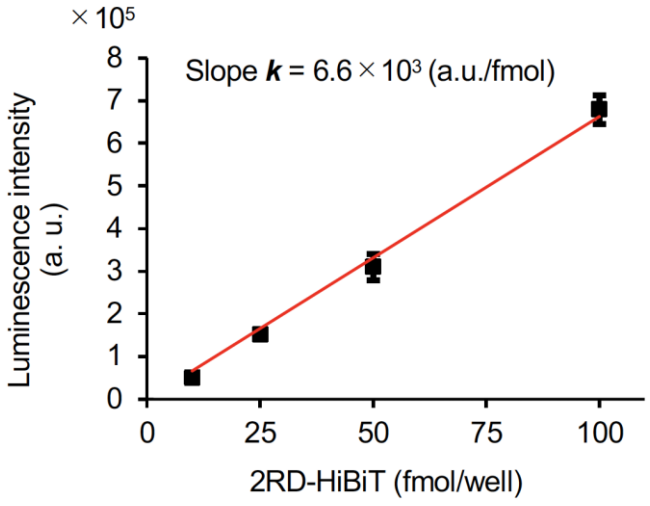

Figure 4. Correlation between 2RD-HiBiT concentration and luminescence generated in the cell lysate assay. Data represent the mean ± standard error (SE; n = 3).

Subsequently, we determined the molar amount of 2RD-HiBiT that reached the cytosol in the presence and absence of L17E. HeLa cells stably expressing LgBiT were incubated with 0.1–1 μM 2RD-HiBiT for 15 min, and the luminescence generated by the binding of LgBiT to 2RD-HiBiT was determined using the Nano-Glo Live Cell Assay System. In the absence of L17E, a gradual 2RD-HiBiT concentration-dependent increase in luminescence was observed (Figure 5A). Using the abovementioned correction coefficient and standard curve, we determined that treatment with 1 μM 2RD-HiBiT yielded approximately 6 fmol of cytosol-localized HiBiT per well in a 96-well plate. Furthermore, using the standard curve with a slope $\boldsymbol{k} = 6.6 \times 10^3$ (a.u./fmol), a cell volume estimate of 3.2 pL ($\boldsymbol{V}$), and a cell number of 2.1×10^4 per well ($\boldsymbol{n}$ in Figure 2D: determined using automated cell counter), we calculated the mean cytosolic 2RD-HiBiT concentration to be approximately 0.09 μM following treatment. Therefore, even though no cytosolic FITC-2RD-HiBiT signal was observed (Figure 3B), it was found that 2RD-HiBiT alone could migrate into the cytosol. A considerable increase in the efficacy of cytosolic translocation was obtained in the presence of 40 μM L17E, yielding a cytosolic 2RD-HiBiT concentration of approximately 0.4 μM, an approximately 6-fold concentration of that obtained in the absence of L17E. Additionally, the concentration of LgBiT expressed in the cytosol was estimated at approximately 10 μM upon the addition of an excess amount of 2RD-HiBiT to the cell lysates (see Supporting Information for experimental details), suggesting that most 2RD-HiBiT delivered into the cytosol formed a complex with LgBiT.

We analyzed the time course of the cytosolic release of 2RD-HiBiT in the presence of L17E and HAad (Figure 5B). A gradual increase in cytosolic 2RD-HiBiT concentration was observed, reaching approximately 0.2 μM at 30 min. A marked increase in cytosolic 2RD-HiBiT concentration was observed in the presence of 40 μM L17E. Notably, L17E delivered 2RD-HiBiT into the cytosol within 5 min, which is consistent with previous reports of IgG delivery by L17E.[11] A cytosolic 2RD-HiBiT concentration of approximately 1 μM was obtained in the presence of L17E. HAad was designed as an improved version of L17E, and delivered cargos such as IgG into the cytosol of more number of cells.[12] In this study, HAad yielded a mean 2RD-HiBiT cytosolic concentration of approximately 1.2 μM; however, statistical analysis revealed no significant difference in the cytosolic concentrations obtained with the use of L17E and HAad.

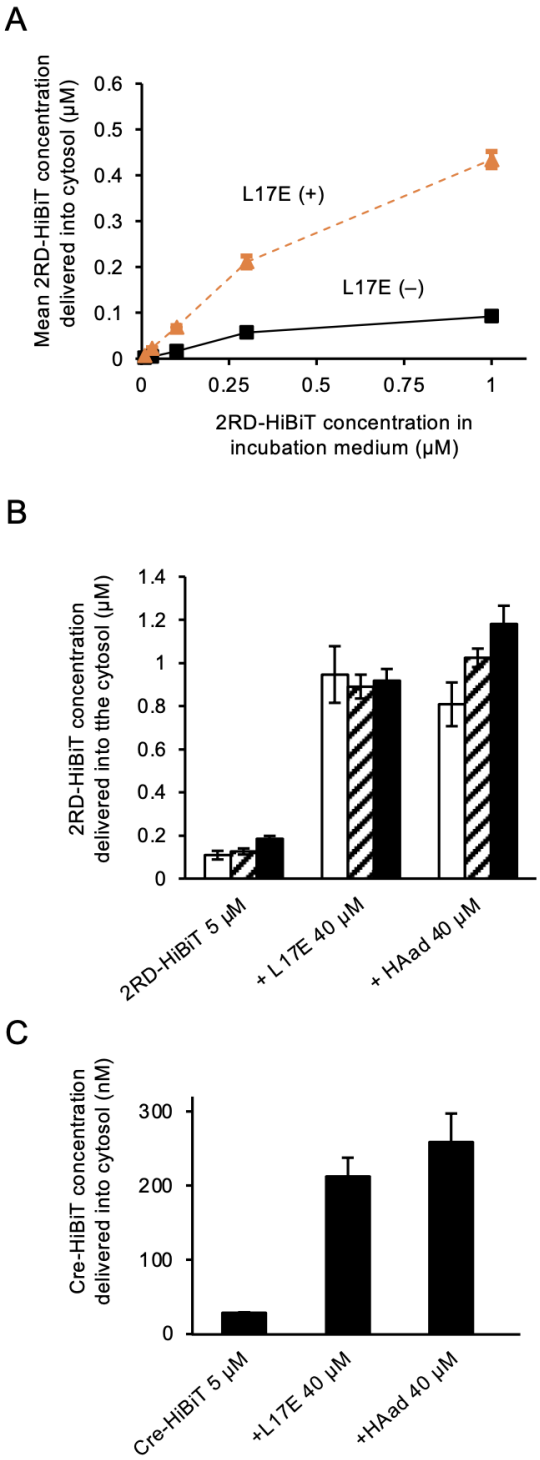

Figure 5. (A) Effect of 2RD-HiBiT and L17E concentrations on the cytosolic translocation of 2RD-HiBiT after a 15-min incubation. (B) Time course of cytosolic translocation of 2RD-HiBiT (5 μM) in the absence or presence of L17E and HAad (40 μM each). Open, hatched, and closed bars represent mean cytosolic 2RD-HiBiT concentrations at 5, 15, and 30 min after peptide addition, respectively. (C) Mean concentrations of Cre-HiBiT delivered into the cytosol via L17E and HAad were obtained using the parameters in Figure 2D ($\boldsymbol{X/Y}$ = 0.68, $\boldsymbol{k}$ = 6.6 × 10^3 a.u./fmol; n = 2.1 × 10^4, and $\boldsymbol{V}$ = 3.2 pL). Data represent the mean ± SE (n = 3).

We investigated whether the system we developed could be used to assess the cytosolic concentration of proteins delivered by these peptides. In our previous study, Cre DNA recombinase was employed as a model cargo.[11,12,33] Therefore, we prepared a Cre-HiBiT fusion protein (Figure S3) and assessed the efficacy of L17E and HAad in stimulating cytosolic translocation of Cre-HiBiT, in a manner similar to that described above. Use of Cre-HiBiT alone resulted in an approximate cytosolic concentration of 0.05 μM, whereas the presence of 40 μM L17E or HAad enhanced this yield to around 0.2–0.3 μM, (Figure 5C), No statistically significant differences were found in the cytosolic cargo concentrations obtained by the treatment with either of the peptides.

More detailed studies are needed to elucidate the underlying mechanisms as to why HAad did not demonstrate a superior ability to deliver the 2RD-HiBiT peptide and Cre-HiBiT protein compared to L17E as reported in our previous study.[12] One possible explanation could be that this study focused on mean cytosolic cargo concentration, whereas HAad superiority was determined based on the number of cells having cytosolic cargo fluorescent signals; microscopic analysis may be less sensitive than chemiluminescent assay especially when cytosolic cargo concentration is relatively low as suggested in the cytosolic localization of 2RD-HiBiT (Figures 3B versus 5B).

In conclusion, we constructed a split luciferase system and demonstrated the feasibility of evaluating and comparing the cytosolic delivery of functional peptides and proteins. We successfully estimated mean cytosolic cargo concentrations using this approach. The use of cells stably expressing LgBiT was recommendable to ensure the reproducibility of the results. Although HeLa cells were employed to show the validity of our approach in this study, the same approach could also be extended to other cell lines stably expressing LgBiT. Our approach did not consider the dispersion of cellular HiBiT concentration, which may differ widely across cells, as exemplified in Figure 3B. Therefore, in this study, we employed the expression of mean cytosolic concentration. Our findings were based on the assumption that most HiBiT segments formed complexes with LgBiT, regardless of the concentration and differences in peptides attached to the HiBiT segment. Further work is required to address these limitations and refine the system we designed. However, we believe that our approach is the first to enable the estimation of rough cytosolic cargo concentration, and the information obtained, would be highly beneficial in designing systems for the delivery of biopharmaceuticals into living cells.

Declaration of Interest

This study was in part funded by Shionogi & Co., Ltd.

Acknowledgments

This work was supported by JSPS KAKENHI (Grant Number JP21H04794) and by JST CREST (Grant Number JPMJCR18H5) to S.F.

Appendix A. Supplementary data

Supplementary data to this article (Materials and Methods, Supplementary Information Figures) can be found online at

References

1 Singh, K., Ejaz, W., Dutta, K. & Thayumanavan, S. Antibody Delivery for Intracellular Targets: Emergent Therapeutic Potential. *Bioconjug Chem* **30**, 1028-1041, doi:10.1021/acs.bioconjchem.9b00025 (2019).

2 Futaki, S., Arafiles, J. V. V. & Hirose, H. Peptide-assisted Intracellular Delivery of Biomacromolecules. *Chemistry Letters* **49**, 1088-1094, doi:10.1246/cl.200392 (2020).

3 Goswami, R., Jeon, T., Nagaraj, H., Zhai, S. & Rotello, V. M. Accessing Intracellular Targets through Nanocarrier-Mediated Cytosolic Protein Delivery. *Trends Pharmacol Sci* **41**, 743-754, doi:10.1016/j.tips.2020.08.005 (2020).

4 Brock, D. J., Kondow-McConaghy, H. M., Hager, E. C. & Pellois, J. P. Endosomal Escape and Cytosolic Penetration of Macromolecules Mediated by Synthetic Delivery Agents. *Bioconjug Chem* **30**, 293-304, doi:10.1021/acs.bioconjchem.8b00799 (2019).

5 El-Sayed, A., Futaki, S. & Harashima, H. Delivery of macromolecules using arginine-rich cell-penetrating peptides: ways to overcome endosomal entrapment. *AAPS J* **11**, 13-22, doi:10.1208/s12248-008-9071-2 (2009).

6 Pei, D. & Buyanova, M. Overcoming Endosomal Entrapment in Drug Delivery. *Bioconjug Chem* **30**, 273-283, doi:10.1021/acs.bioconjchem.8b00778 (2019).

7 Smith, S. A., Selby, L. I., Johnston, A. P. R. & Such, G. K. The Endosomal Escape of Nanoparticles: Toward More Efficient Cellular Delivery. *Bioconjug Chem* **30**, 263-272, doi:10.1021/acs.bioconjchem.8b00732 (2019).

8 Peng, L. & Wagner, E. Polymeric Carriers for Nucleic Acid Delivery: Current Designs and Future Directions. *Biomacromolecules* **20**, 3613-3626, doi:10.1021/acs.biomac.9b00999 (2019).

9 Porosk, L., Gaidutšik, I. & Langel, Ü. Approaches for the discovery of new cell-penetrating peptides. *Expert Opin Drug Discov* **16**, 553-565, doi:10.1080/17460441.2021.1851187 (2021).

10 Martinek, T. A. & Fülöp, F. Peptidic foldamers: ramping up diversity. *Chem Soc Rev* **41**, 687-702, doi:10.1039/c1cs15097a (2012).

11 Akishiba, M. *et al.* Cytosolic antibody delivery by lipid-sensitive endosomolytic peptide. *Nat Chem* **9**, 751-761, doi:10.1038/nchem.2779 (2017).

12 Sakamoto, K. *et al.* Optimizing Charge Switching in Membrane Lytic Peptides for Endosomal Release of Biomacromolecules. *Angew Chem Int Ed Engl* **59**, 19990-19998, doi:10.1002/anie.202005887 (2020).

13 Futaki, S. Functional Peptides That Target Biomembranes: Design and Modes of

Action. *Chem Pharm Bull (Tokyo)* **69**, 601-607, doi:10.1248/cpb.c21-00140 (2021).

14 Futaki, S. & Nakase, I. Cell-Surface Interactions on Arginine-Rich Cell-Penetrating Peptides Allow for Multiplex Modes of Internalization. *Acc Chem Res* **50**, 2449-2456, doi:10.1021/acs.accounts.7b00221 (2017).

15 Kosuge, M., Takeuchi, T., Nakase, I., Jones, A. T. & Futaki, S. Cellular internalization and distribution of arginine-rich peptides as a function of extracellular peptide concentration, serum, and plasma membrane associated proteoglycans. *Bioconjug Chem* **19**, 656-664, doi:10.1021/bc700289w (2008).

16 Burlina, F., Sagan, S., Bolbach, G. & Chassaing, G. A direct approach to quantification of the cellular uptake of cell-penetrating peptides using MALDI-TOF mass spectrometry. *Nat Protoc* **1**, 200-205, doi:10.1038/nprot.2006.30 (2006).

17 Bernal, F., Tyler, A. F., Korsmeyer, S. J., Walensky, L. D. & Verdine, G. L. Reactivation of the p53 tumor suppressor pathway by a stapled p53 peptide. *J Am Chem Soc* **129**, 2456-2457, doi:10.1021/ja0693587 (2007).

18 Lönn, P. *et al.* Enhancing Endosomal Escape for Intracellular Delivery of Macromolecular Biologic Therapeutics. *Sci Rep* **6**, 32301, doi:10.1038/srep32301 (2016).

19 Schmidt, S. *et al.* Detecting Cytosolic Peptide Delivery with the GFP Complementation Assay in the Low Micromolar Range. *Angew Chem Int Ed Engl* **54**, 15105-15108, doi:10.1002/anie.201505913 (2015).

20 Milech, N. *et al.* GFP-complementation assay to detect functional CPP and protein delivery into living cells. *Sci Rep* **5**, 18329, doi:10.1038/srep18329 (2015).

21 Teo, S. L. Y. *et al.* Unravelling cytosolic delivery of cell penetrating peptides with a quantitative endosomal escape assay. *Nat Commun* **12**, 3721, doi:10.1038/s41467-021-23997-x (2021).

22 Nomura, W., Ohashi, N., Mori, A. & Tamamura, H. An in-cell fluorogenic Tag-probe system for protein dynamics imaging enabled by cell-penetrating peptides. *Bioconjug Chem* **26**, 1080-1085, doi:10.1021/acs.bioconjchem.5b00131 (2015).

23 Qian, Z. *et al.* Efficient delivery of cyclic peptides into mammalian cells with short sequence motifs. *ACS Chem Biol* **8**, 423-431, doi:10.1021/cb3005275 (2013).

24 Lee, Y. J., Datta, S. & Pellois, J. P. Real-time fluorescence detection of protein transduction into live cells. *J Am Chem Soc* **130**, 2398-2399, doi:10.1021/ja7102026 (2008).

25 Peraro, L. *et al.* Cell Penetration Profiling Using the Chloroalkane Penetration Assay. *J Am Chem Soc* **140**, 11360-11369, doi:10.1021/jacs.8b06144 (2018).

26 Borra, R., Dong, D., Elnagar, A. Y., Woldemariam, G. A. & Camarero, J. A. In-cell fluorescence activation and labeling of proteins mediated by FRET-quenched split inteins. *J Am Chem Soc* **134**, 6344-6353, doi:10.1021/ja300209u (2012).

27 Lucchino, M. *et al.* Absolute Quantification of Drug Vector Delivery to the Cytosol. *Angew Chem Int Ed Engl* **60**, 14824-14830, doi:10.1002/anie.202102332 (2021).

28 LaRochelle, J. R., Cobb, G. B., Steinauer, A., Rhoades, E. & Schepartz, A. Fluorescence correlation spectroscopy reveals highly efficient cytosolic delivery of certain penta-arg proteins and stapled peptides. *J Am Chem Soc* **137**, 2536-2541, doi:10.1021/ja510391n (2015).

29 Dixon, A. S. *et al.* NanoLuc Complementation Reporter Optimized for Accurate Measurement of Protein Interactions in Cells. *ACS Chem Biol* **11**, 400-408, doi:10.1021/acschembio.5b00753 (2016).

30 England, C. G., Ehlerding, E. B. & Cai, W. NanoLuc: A Small Luciferase Is Brightening Up the Field of Bioluminescence. *Bioconjug Chem* **27**, 1175-1187, doi:10.1021/acs.bioconjchem.6b00112 (2016).

31 Takayama, K. *et al.* Enhanced intracellular delivery using arginine-rich peptides by the addition of penetration accelerating sequences (Pas). *Journal of Controlled Release* **138**, 128-133, doi:10.1016/j.jconrel.2009.05.019 (2009).

32 Jullian, M. *et al.* N-terminus FITC labeling of peptides on solid support: the truth behind the spacer. *Tetrahedron Letters* **50**, 260-263, doi: 10.1016/j.tetlet.2008.10.141 (2009).

33 Arafiles, J. V. V. *et al.* Stimulating Macropinocytosis for Intracellular Nucleic Acid and Protein Delivery: A Combined Strategy with Membrane-Lytic Peptides To Facilitate Endosomal Escape. *Bioconjug Chem* **31**, 547-553, doi:10.1021/acs.bioconjchem.0c00064 (2020).